Decoupling transition of flux lattices in pure layered superconductors

Ruth Goldin[1] and Baruch Horovitz[1,2]
[1]*Department of Physics, Ben-Gurion University of the Negev, Beer-Sheva 84105, Israel*
[2]*Ilze Katz Center for Nanotechnology, Ben-Gurion University of the Negev, Beer-Sheva 84105, Israel*
(Received 29 April 2004; revised manuscript received 16 March 2005; published 14 July 2005)

We study the decoupling transition of flux lattices in layered superconductors at which the Josephson coupling J is renormalized to zero. We identify the order parameter and related correlations; the latter are shown to decay as a power law in the decoupled phase. Within the second-order renormalization group we find that the transition is always continuous, in contrast with results of the self-consistent harmonic approximation. The critical temperature for weak J is $\sim 1/B$, where B is the magnetic field, while for strong J it is $\sim 1/\sqrt{B}$ and is strongly enhanced. We show that renormaliztion group can be used to evaluate the Josephson plasma frequency and find that for weak J it is $\sim 1/BT^2$ in the decoupled phase.

DOI: 10.1103/PhysRevB.72.024518 PACS number(s): 74.25.Qt, 74.25.Dw, 74.50.+r

I. INTRODUCTION

In many aspects the behavior of the high-temperature superconductors in the mixed state differs from that of conventional superconductors. A combination of elevated critical temperatures, high anisotropy, and short superconducting coherence lengths considerably enhance the role of fluctuations on the vortex interaction, which result in a noticeable change in the nature of the mixed state.

The phase diagram of these layered superconductors in a magnetic field B perpendicular to the layers has been studied in considerable detail.[1] A first-order transition in $YBa_2Cu_3O_7$ (YBCO) and in $Bi_2Sr_2CaCu_2O_8$ (BSCCO) has been interpreted as a flux lattice melting. The data suggests that the first order line terminates at a multicritical point, which for BSCCO is at $B_0 \approx 300-10^3$ G and at temperatures, $T_0 \approx 40-50$ K[2,3] while for YBCO (Ref. 4) it is at $B_0 \approx 2-10$ T and $T_0 \approx 60-80$ K, depending on disorder and oxygen concentration. At low temperatures as B is increased a "second peak" transition is manifested as a sharp increase in magnetization. The second peak transition is at $B \approx B_0$ starting from the critical point; it is weakly temperature dependent and shifts to lower fields with increasing disorder.[2] More recent data on BSCCO (data) show,[5] however, that the second peak line connects smoothly with the first order line; the presence of a multicritical point depends then on the possibility that an additional line joins in the high field regime. Josephson plasma resonance studies[6,7] have shown a significant reduction of the Josephson coupling at the second peak transition. The combination of reduced Josephson coupling and enhanced pinning indicates an unusual phase transition.

The flux lattice can undergo a transition which is unique to a layered superconductor, i.e., a decoupling transition.[8–11] In this transition the Josephson coupling between layers vanishes while the lattice is maintained by the magnetic coupling. The theory of Daemen *et al.*[10] employed the method of self-consistent harmonic approximation (SCHA) to find the decoupling temperature $T_d(B)$. The SCHA leads to a conceptual difficulty since it predicts that the average $\langle \cos \phi \rangle$, where ϕ is the Josephson phase, vanishes at $T > T_d$. Koshelev has shown[12] that $\langle \cos \phi \rangle$ is finite at all temperatures and in fact accounts for the experimentally observed Josephson plasma resonance at high temperatures. Thus the decoupling transition, as found by SCHA, needs to be reinterpreted. The correct order parameter is in fact a nonlocal one [Eq. (28) below] and corresponds to the helicity modulus[13] or to the critical current.[12]

In the present work we expand our earlier presentation[14] and study the decoupling transition by second-order renormalization group (RG). Section II defines the model and its effective Hamiltonian. In Sec. III we identify the order parameter and related correlations and show that the latter decay either exponentially in the coupled phase or as a power law in the decoupled phase. We also show that RG can be used to evaluate $\langle \cos \phi \rangle$ and hence the Josephson plasma frequency and predict its behavior in the decoupled phase (Sec. V).

Our RG analysis (Sec. IV) shows that the decoupling transition is continuous in the whole parameter range , in contrast with the SCHA result that it is first order above some critical value of the Josephson coupling.[10] We trace the latter result to a deficiency of the SCHA which does not allow for a scale dependent effective mass (Sec. VI).

Our analysis assumes that point defects like vacancies and interstitials (*V-I*) of the flux lattice are not present. In general, however, *V-I* defects are a relevant perturbation at decoupling.[15,16] The effect is rather weak for actual system parameters, as discussed in Sec. VII.

The role of point disorder on the decoupling has been studied separately[14,17] and in more detail in a companion article.[18] This study shows that disorder induced decoupling leads to an apparent discontinuity in the tilt modulus which then leads to an enhanced critical current and reduced domain size. These results are in accord with the Josephson plasma resonance[6,7] and other data on the second peak transition. Of further interest is the effect of columnar defects on the decoupling transition,[19] an effect which can further identify this transition.

II. THE MODEL

Consider a layered superconductor with a magnetic field perpendicular to the layers. The flux lattice can be considered as point vortices in each superconducting layer which are stacked one on top of the other. Each point vortex, or a pancake vortex, represents a singularity of the superconducting order parameter, i.e., the order parameter's phase in a given layer changes by 2π around the pancake vortex. These pancake vortices are coupled by their magnetic field as well as by the Josephson coupling between nearest layers.

The basic model for studying layered superconductors is the Lawrence-Doniach[20] Hamiltonian in terms of superconducting phases $\varphi_n(\mathbf{r})$ on the nth layer and the vector potential $\mathbf{A}(\mathbf{r},z), A_z(\mathbf{r},z)$ (vectors such as $\mathbf{A}$ and $\mathbf{r}$ are two-dimensional parallel to the layers):

$$\mathcal{H}^{\mathrm{LD}} = \frac{1}{8\pi}\int d^2\mathbf{r}dz\Bigg[[\nabla\times\mathbf{A}(\mathbf{r},z)]^2 + \frac{d}{\lambda_{ab}^2}\sum_n\left(\frac{\Phi_0}{2\pi}\nabla\varphi_n(\mathbf{r})-\mathbf{A}(\mathbf{r},z)\right)^2\delta(z-nd)\Bigg] - \tilde{J}/\xi^2\sum_n\int d^2\mathbf{r}\cos\Bigg[\varphi_n(\mathbf{r})-\varphi_{n-1}(\mathbf{r}) - \frac{2\pi}{\Phi_0}\int_{(n-1)d}^{nd}A_z(\mathbf{r},z)dz\Bigg], \tag{1}$$

where λ_{ab} and ξ are the penetration length and coherence length parallel to the layers, respectively, d is the spacing between layers and $\Phi_0 = hc/2e$ is the flux quantum. The first term in Eq. (1) is the magnetic energy, the second is the supercurrent energy, while the last one is the Josephson coupling where $\tilde{J}$ is the Josephson coupling energy per area ξ^2 between neighboring layers. The model Eq. (1) qualifies as the standard model for layered superconductors.

In this section we outline the derivation of an effective Hamiltonian, which is the basis for RG analysis in the next section. The partition sum for Eq. (1) involves integrating over both $\varphi_n(\mathbf{r})$ and $\mathbf{A}(\mathbf{r},z)$, subject to a gauge condition. Since $\mathbf{A}(\mathbf{r},z)$ is a Gaussian field [choosing the axial gauge $A_z(\mathbf{r},z)=0$] we can shift $\mathbf{A}\to\mathbf{A}+\delta\mathbf{A}$ where $\mathbf{A}(\mathbf{r},z)$ now satisfies the saddle point equations for its x,y components

$$\nabla\times\nabla\times\mathbf{A}(\mathbf{r},z) = \frac{d}{\lambda_{ab}^2}\sum_n\left[\frac{\Phi_0}{2\pi}\nabla\varphi_n(\mathbf{r})-\mathbf{A}(\mathbf{r},z)\right]\delta(z-nd) \tag{2}$$

and then fluctuations in $\delta\mathbf{A}$ decouple from those of $\phi_n(\mathbf{r})$. The partition sum at temperature T involves therefore integration only on the $\phi_n(\mathbf{r})$ variables

$$\mathcal{Z} = \int\mathcal{D}\phi_n(\mathbf{r})\exp[-\mathcal{H}^{\mathrm{LD}}/T] \tag{3}$$

with $\mathbf{A}(\mathbf{r},z)$ in Eq. (1) given by the solution of Eq. (2) for each configuration of $\phi_n(\mathbf{r})$. Note that since Eq. (2) is gauge invariant under $\mathbf{A}\to\mathbf{A}-(\Phi_0/2\pi)\nabla\chi(\mathbf{r},nd)$ and $\varphi_n(\mathbf{r})\to\varphi_n(\mathbf{r})-\chi(\mathbf{r},nd)$ one can, in fact, choose any gauge.

We now decompose $\varphi_n(\mathbf{r})$ to

$$\varphi_n(\mathbf{r}) = \varphi_n^0(\mathbf{r}) + \sum_{\mathbf{r}'}s_n(\mathbf{r}')\alpha(\mathbf{r}-\mathbf{r}'), \tag{4}$$

$$\theta_n(\mathbf{r}) = \varphi_n^0(\mathbf{r}) - \varphi_{n-1}^0(\mathbf{r}), \tag{5}$$

where $\varphi_n^0(\mathbf{r})$ is the nonsingular part of $\varphi_n(\mathbf{r}), \alpha(\mathbf{r}) = \arctan(r_2/r_1)$ is the angle at $\mathbf{r}=(r_1,r_2)$, $s_n(\mathbf{r})=1$ at pancake vortex sites, and $s_n(\mathbf{r})=0$ otherwise. The sum in Eq. (4) is then a sum on $\mathbf{r}'$ being the possible vortex positions on the nth layer, e.g., a grid with spacing ξ.

Solving Eq. (2) for $\mathbf{A}$ in terms of $\theta_n(\mathbf{r})$ and s_n, substituting in Eq. (1) yields after a straightforward analysis the equivalent Hamiltonian[22]

$$\mathcal{H}^{(1)} = \mathcal{H}_v + \mathcal{H}_J + \mathcal{H}_f, \tag{6}$$

where $\mathcal{H}_v$ is the vortex-vortex interaction via the 3D magnetic field, $\mathcal{H}_J$ is interlayer Josephson coupling, and $\mathcal{H}_f$ is an energy due to fluctuations of the nonsingular phase

$$\mathcal{H}_v = \frac{1}{2}\sum_{r,n}\sum_{r',n'}s_n(\mathbf{r})G_v(\mathbf{r}-\mathbf{r}';n-n')s_{n'}(\mathbf{r}'), \tag{7}$$

$$\mathcal{H}_J = -\frac{\tilde{J}}{\xi^2}\sum_n\int d^2\mathbf{r}\times\left(\cos\left[\theta_n(\mathbf{r})+\sum_{\mathbf{r}'}[s_n(\mathbf{r}')-s_{n-1}(\mathbf{r}')]\alpha(\mathbf{r}-\mathbf{r}')\right]-1\right), \tag{8}$$

$$\mathcal{H}_f = \frac{1}{2}\int\frac{d^2qdk}{(2\pi)^3}G_f^{-1}(q,k)|\theta(\mathbf{q},k)|^2. \tag{9}$$

Here $(\mathbf{q},k)$ is a 3D wave vector which is the Fourier transform to $\mathbf{r},z$ with $|q|<1/\xi$ and $|k|<\pi/d$, and

$$G_v(q,k) = \frac{\Phi_0^2d^2}{4\pi\lambda_{ab}^2}\frac{1}{q^2}\frac{1}{1+f(q,k)}, \tag{10}$$

$$f(q,k) = \frac{d}{4\lambda_{ab}^2q}\frac{\sinh qd}{\sinh^2\frac{qd}{2}+\sin^2\frac{kd}{2}}, \tag{11}$$

$$G_f(q,k) = \frac{16\pi^3d^2}{\Phi_0^2q^2}\left(1+\frac{4\lambda_{ab}^2}{d^2}\sin^2\frac{kd}{2}\right). \tag{12}$$

Consider now a flux lattice with equilibrium positions $\mathbf{R}_l$ (e.g., a hexagonal lattice) where l labels the flux lines. The actual positions of the pancake vortices deviate from the perfect lattice positions by $\mathbf{u}_l^n$ on the nth layer. The function $s_n(\mathbf{r})$ is then

$$s_n(\mathbf{r}) = \begin{cases}1 & \text{if } \mathbf{r}=\mathbf{R}_l+\mathbf{u}_l^n,\\ 0 & \text{otherwise.}\end{cases}$$

The Fourier transform

$$\mathbf{u}(\mathbf{q},k) = \sum_{n,l}\mathbf{u}_l^n\exp(i\mathbf{q}\cdot\mathbf{R}_l+iknd)$$

identifies longitudinal $u^l(\mathbf{q},k)=\mathbf{q}\cdot\mathbf{u}(\mathbf{q},k)/q$ and transverse $u^{\mathrm{tr}}(\mathbf{q},k)=[\mathbf{q}\times\hat{z}]\cdot\mathbf{u}(\mathbf{q},k)/q$ components of $\mathbf{u}(\mathbf{q},k)$

$$\mathbf{u}(\mathbf{q},k) = u^l(\mathbf{q},k)\mathbf{q}/q + u^{\mathrm{tr}}(\mathbf{q},k)[\mathbf{q}\times\hat{z}]/q,$$

where $\hat{z}$ is a unit vector in the z direction. The inverse transform is

$$\mathbf{u}_l^n = a^2 d\int_{q,k}\mathbf{u}(\mathbf{q},k)e^{-i\mathbf{q}\cdot\mathbf{R}_l - iknd}, \tag{13}$$

where $\int_{q,k}=\int_{\mathrm{BZ}}d^2q dk/(2\pi)^3$, $\int_{\mathrm{BZ}}$,is the $\mathbf{q}$ integration over the Brillouin zone (of area $4\pi^2/a^2$) while $|k|<\pi/d$, and a^2 is the area of the flux lattice's unit cell. Note that $\theta(\mathbf{q},k)$ involves much higher q components, up to the cutoff $1/\xi$.

The next step is to consider small displacements in F_v, Eq. (7); this is equivalent to assuming that the temperature is well below the melting temperature T_m. This expansion identifies the magnetic contribution to the elastic constants, leading to a Hamiltonian of the form

$$\begin{aligned}\mathcal{H}^{(2)} &= \frac{1}{2}(da^2)^2\int_{q,k}\left[q^2 c_{66}^0 + k_z^2 c_{44}^0(k)\right]|u^{\mathrm{tr}}(\mathbf{q},k)|^2 + \mathcal{H}_{\mathrm{el}}\{u^l(\mathbf{q},k)\}\\ &+ \frac{1}{2}\int^{1/\xi}\frac{d^2\mathbf{q}dk}{(2\pi)^3}G_f^{-1}(q,k)|\theta(\mathbf{q},k)|^2\\ &- (\tilde{J}/\xi^2)\sum_n\int d^2\mathbf{r}\cos\Big(\theta_n(\mathbf{r}) + \sum_l[\alpha(\mathbf{r}-\mathbf{R}_l-\mathbf{u}_l^n)\\ &- \alpha(\mathbf{r}-\mathbf{R}_l-\mathbf{u}_l^{n+1})]\Big),\end{aligned} \tag{14}$$

where $\mathcal{H}_{\mathrm{el}}\{u^l(\mathbf{q},k)\}$ involves elastic constants of the longitudinal modes and $k_z^2=(4/d^2)\sin^2(kd/2)$. The elastic constants for the transverse modes, excluding Josephson coupling terms, are given by[9,23]

$$c_{44}^0(k) = \frac{\tau}{8da^2\lambda_{ab}^2}\frac{1}{k_z^2}\ln\frac{1+k_z^2/Q_0^2}{1+\xi^2k_z^2}, \tag{15}$$

$$c_{66}^0 = \frac{\tau}{16da^2}, \tag{16}$$

where $Q_0^2=4\pi B/\Phi_0=4\pi/a^2$, i.e., πQ_0^2 is the area of a Brillouin zone, and

$$\tau = \frac{\Phi_0^2 d}{4\pi^2\lambda_{ab}^2}. \tag{17}$$

If the Josephson term is expanded it would add more terms to the elastic constants, however, near decoupling the nonlinearity of the term is essential.

We can estimate the condition $T\ll T_m$ by evaluating the melting temperature via the Lindeman criterion $\langle(u_l^n)^2\rangle_0 \approx c_L^2 a^2$ where c_L is a Lindeman number of order 0.15 and the average is with respect to the elastic terms. The average is dominated by the softer transverse modes yielding $T_m\ln(2\pi^2\lambda_{ab}^2/a^2)\approx c_L^2\tau$, i.e., τ is the temperature scale for melting. Melting in the absence of Josephson coupling was in fact studied[21], showing that T_m is between $\tau/8$ and the two-dimensional melting temperature $\approx 0.004\tau$, approaching the latter at high fields $a\ll\lambda_{ab}$. The condition $T_d\ll T_m$ is in fact satisfied only at $a\ll\lambda_{ab}$ [Eqs. (50), (65), and (66) below], hence we limit our solutions to $T_d \lesssim 0.01\tau$.

The next simplification, in accord with the condition of small displacements $|u_l^n|\ll a$ is an expansion of the relative phase in the Josephson term:

$$\begin{aligned}\sum_l[\alpha(\mathbf{r}-\mathbf{R}_l-\mathbf{u}_l^n) - \alpha(\mathbf{r}-\mathbf{R}_l-\mathbf{u}_l^{n+1})] &\simeq \sum_l(\mathbf{u}_l^{n+1}-\mathbf{u}_l^n)\cdot\nabla\alpha(\mathbf{r}-\mathbf{R}_l^n)\\ &\equiv \tilde{b}_n(\mathbf{r}).\end{aligned} \tag{18}$$

Since $\tilde{b}_n(\mathbf{r})$ contains all $\mathbf{q}$ in its Fourier transform it is useful to separate from it the components within the first Brillouin zone

$$\begin{aligned}\tilde{b}_n(\mathbf{r}) &= b_n(\mathbf{r}) + B_n(\mathbf{r})b_n(\mathbf{r})\\ &= 2\pi id\int_{\mathrm{BZ}}\frac{d^2\mathbf{q}dk}{(2\pi)^3}e^{-i\mathbf{q}\cdot\mathbf{r}-iknd}(e^{ikd}-1)\frac{u^{\mathrm{tr}}(\mathbf{q},k)}{\mathbf{q}}B_n(\mathbf{r})\\ &= 2\pi id\sum_{\mathbf{Q}\neq 0}\int_{\mathrm{BZ}}\frac{d^2\mathbf{q}dk}{(2\pi)^3}e^{-i(\mathbf{q}+\mathbf{Q})\cdot\mathbf{r}-iknd}(e^{ikd}-1)\\ &\times\frac{\mathbf{u}(\mathbf{q},k)\cdot[\hat{z}\times(\mathbf{q}+\mathbf{Q})]}{(\mathbf{q}+\mathbf{Q})^2}.\end{aligned} \tag{19}$$

The last term displays the Fourier transform of $\nabla\alpha(\mathbf{r})$, which for $Q=0$ projects the transverse displacement.

The lowest order effect of thermal fluctuations is obtained as an average with respect to the elastic terms, i.e.,

$$\langle\cos[\theta_n(\mathbf{r})+\tilde{b}_n(\mathbf{r})]\rangle_0 = \exp\left[-\frac{1}{2}\langle\theta_n^2(\mathbf{r})\rangle_0 - \frac{1}{2}\langle\tilde{b}_n^2(\mathbf{r})\rangle_0\right]. \tag{20}$$

The only singular term in this average is due to $b_n(\mathbf{r})$ from Eq. (19) which in fact drives the decoupling transition, i.e. even if the fluctuations in u_l^n are small, their effect on the Josephson phase can be divergent. The average $\langle B_n^2(\mathbf{r})\rangle_0$ is readily shown to yield $\approx T/\tau$, up to logarithmic terms, and since $T\ll\tau$ below melting its effect in Eq.(20) is negligible.

We wish to integrate out also the high $\mathbf{q}$ modes of $\theta(\mathbf{q},k)$, i.e., momenta in the range $Q_0<q<1/\xi$. The effect from Eq. (20) is a factor

$$D = e^{(-1/2)\int_{1/a}^{1/\xi}d^2q dk G_f(q,k)/(2\pi)^3} = e^{-(T/\tau)\ln(a/\xi)}$$

which can also be neglected.

The effective Hamiltonian is now defined with a momentum cutoff $q<Q_0$ and the corresponding smallest length scale is a. The Josephson term involves $J\Sigma_r\rightarrow(J/a^2)\int d^2r$ so that J is now the Josephson coupling energy per area a^2, i.e., $J=\tilde{J}(a/\xi)^2$. Since $b_n(\mathbf{r})$ depends only on the transverse modes all longitudinal terms are decoupled and we can consider an effective Hamiltonian for the transverse modes

$$\mathcal{H}^{(3)} = \frac{1}{2}\sum_{\mathbf{q},k}\left[G_f^{-1}(q,k)|\theta(\mathbf{q},k)|^2 + G_b^{-1}(q,k)|b(\mathbf{q},k)|^2\right] - (J/a^2)\sum_n \int d^2\mathbf{r}\cos[\theta_n(\mathbf{r}) + b_n(\mathbf{r})] \quad (21)$$

where

$$G_b^{-1}(q,k) = q^2\frac{a^4}{(2\pi d)^2}[c_{44}^0 + q^2 c_{66}^0/k_z^2]. \quad (22)$$

Finally we shift

$$\phi_n(\mathbf{r}) = b_n(\mathbf{r}) + \theta_n(\mathbf{r})$$

so that $\theta(\mathbf{q},k)$ can be integrated out leading to a Gaussian term $\frac{1}{2}\Sigma_{\mathbf{q},k}[G_b(q,k)+G_f(q,k)]^{-1}|\phi(\mathbf{q},k)|^2$. It is readily shown that $G_f(q,k)/G_b(q,k) \ll 1$ for all $\mathbf{q},k$, except when both $k < 1/\lambda_{ab}$ and $q \gg k\lambda_{ab}/a$ which has negligible effect since large k dominates the following integrals. Therefore we neglect $G_f(q,k)$ and our final Hamiltonian is

$$\mathcal{H} = \frac{1}{2}\sum_{\mathbf{q},k} G_b^{-1}(q,k)|\phi(\mathbf{q},k)|^2 - (J/a^2)\sum_n \int d^2\mathbf{r}\cos\phi_n(\mathbf{r}), \quad (23)$$

Our task is then to evaluate the partition sum

$$\mathcal{Z} = \int \mathcal{D}\phi e^{-\mathcal{H}\{\phi\}/T}. \quad (24)$$

III. GENERAL PROPERTIES

In this section we identify the order parameter of the decoupling transition and related correlation functions. Also a scheme for evaluating the frequency of the Josephson plasma resonance is given.

In the RG procedure, as detailed in Sec. IV, a phase transition is found at a temperature T_d such that at $T > T_d J$ is irrelevant (scales to zero under RG) while at $T < T_d$ it is relevant (scales to strong coupling). To identify the order parameter of this transition we consider first the Hamiltonian Eq. (23) in presence of an external vector potential in the z direction $A_n(\mathbf{r})$ which is z independent between layers. The relative superconducting phase on neighboring layers $\phi_n(\mathbf{r})$ is then shifted by $(2\pi d/\phi_0)A_n(\mathbf{r})$ and the Hamiltonian becomes

$$\mathcal{H}_{\mathcal{A}} = \frac{1}{2}\sum_{\mathbf{q},k} G_b^{-1}(q,k)|\phi(\mathbf{q},k)|^2 - (J/a^2)\sum_n \int d^2\mathbf{r}\cos\left[\phi_n(\mathbf{r}) - \frac{2\pi d}{\phi_0}A_n(\mathbf{r})\right]. \quad (25)$$

The Josephson current is a derivative of the free energy $\mathcal{F} = -T\ln\mathcal{Z}$

$$j_z(\mathbf{r},n) = -\frac{c}{d}\frac{\partial\mathcal{F}}{\partial A_n(\mathbf{r})} = \frac{2\pi c}{\phi_0}\frac{J}{a^2}\left\langle \sin\left[\phi_n(\mathbf{r}) - \frac{2\pi d}{\phi_0}A_n(\mathbf{r})\right]\right\rangle_A. \quad (26)$$

The linear response to $A_n(\mathbf{r})$ has a $\sim\cos\phi_n(\mathbf{r})$ term as well as a nonlocal term from the expansion of $\mathcal{H}_{\mathcal{A}}$ in $\exp(-\mathcal{H}_{\mathcal{A}}/T)$,

$$j_z(\mathbf{r},n) = -\left(\frac{2\pi}{\phi_0}\right)^2\frac{Jdc}{a^2}\left[\langle\cos\phi_n(\mathbf{r})\rangle A_n(\mathbf{r}) - \frac{J}{Ta^2}\sum_{n'}\int d^2r'\langle\sin\phi_n(\mathbf{r})\sin\phi_{n'}(\mathbf{r}')\rangle A_{n'}(\mathbf{r}')\right], \quad (27)$$

where averages $\langle\cdots\rangle$ are in the $A=0$ system. The superconducting response is identified by a uniform $A_n(\mathbf{r})=A$ so that the superconducting phase $\varphi_n(\mathbf{r})$ acquires a uniform twist $\varphi_n(\mathbf{r}) - (2\pi/\phi_0)An$. Note that the partition sum excludes $\varphi_n(\mathbf{r})$ with a global twist, hence the A term cannot be transformed away. The superconducting response Q is defined by $j_n(\mathbf{r}) = QA$, i.e.,

$$Q = \left(\frac{2\pi}{\phi_0}\right)^2\frac{Jdc}{a^2} \times \left[\langle\cos\phi\rangle - \frac{J}{Ta^2}\sum_n\int d^2r\langle\sin\phi_0(0)\sin\phi_n(\mathbf{r})\rangle\right], \quad (28)$$

where $\langle\cos\phi_n(\mathbf{r})\rangle$ is n and $\mathbf{r}$ independent is written for short as $\langle\cos\phi\rangle$. This order parameter was identified by Li and Teitel[13] as a helicity modulus and by Koshelev[12] as the superconducting response [i.e., the zero frequency limit of his Eq. (3)]. This order parameter signifies breaking of gauge symmetry: at $T > T_d$ the irrelevancy of J implies diverging fluctuations in $\phi_n(\mathbf{r})$, hence $A_n(\mathbf{r})$ has no effect on Z and $Q = 0$. At $T < T_d J$ flows to strong coupling so that $\phi_n(\mathbf{r})$ has finite fluctuations near the energy minimum where $\phi_n(\mathbf{r}) = 0$; this implies that a gauge transformation of $A_n(\mathbf{r})$ must be combined with a change in $\phi_n(\mathbf{r})$. The manifestation of this broken gauge symmetry is $Q \neq 0$ or a finite Josephson current.

The Josephson plasma resonance frequency ω_{pl} is a significant probe[6,7] of a possible decoupling transition. As shown by Koshelev[12] the superconducting response at ω_{pl} is dominated by the 1st term of Eq. (28), so that $\omega_{\mathrm{pl}} \sim \langle\cos\phi\rangle$. We reconsider this relation in Sec. V while here we present a scheme for evaluating $\langle\cos\phi\rangle$. We note first that a derivative of the free energy yields

$$\langle\cos\phi\rangle = \frac{a^2}{NL^2}\frac{\partial}{\partial J}\mathcal{F}(J), \quad (29)$$

where L^2 is a layer area and N is the number of layers. While the details of the RG procedure are not needed in this section, some general properties can be derived from the asymptotic RG transformation. A general RG changes the original lattice unit a to a renormalized one a^R while $J(a) \to J(a^R)=J^R$; additional parameters in $\mathcal{F}(J)$ (not displayed here) may also be renormalized while $\mathcal{F}$ itself changes by

$$d\mathcal{F} = -NL^2 f(a)da, \quad (30)$$

In first-order RG $f(a)=0$ (Sec. IV A) but becomes finite in second order (section IV B) so that $f(a) \sim J^2(a)$. Hence integrating Eq. (30) yields a J dependent term for either a relevant or irrelevant y, hence $\langle \cos \phi \rangle$ is finite in either the coupled or the decoupled phases. We consider in particular the decoupled phase $T > T_d$ and a system size $L \gg a$. At the final stage of RG when $a^R \to L$ the renormalized J^R becomes extremely small and one can safely use 1st order RG which has the form (Sec. IV A)

$$dJ/J = 2(1-Z)da/a, \quad (31)$$

where $Z=Z(J,T)$ contains renormalizations due to higher order RG terms at shorter scales; note that $Z=1$ at $T=T_d$ since for $Z>1$ Eq. (31) shows that $J^R \sim L^{2(1-Z)} \to 0$ at $L \to \infty$. E.g. if 1st order RG is used all the way from the initial values then $Z=T/T_d^0$ where T_d^0 is Eq. (44) below. Integrating Eq. (30) yields

$$F(J^R) - F(J) = -NL^2 \int_a^{a^R} f(a')da'. \quad (32)$$

At the scale $a^R=L$ the system has just one degree of freedom so that the term $\sim q^2\phi(\mathbf{q},k)$ in Eq. (23) is absent, hence

$$F(J^R) = -T \ln\left[\int_0^{2\pi} d\phi e^{J^R \cos \phi/T}\right]^N = -\frac{1}{4}TN\left[\left(\frac{J^R}{T}\right)^2 + O\left(\frac{J^R}{T}\right)^4\right]. \quad (33)$$

Thus $F(J^R) \sim L^{4(1-Z)}$ at $T>T_d$ so that at $L \to \infty$

$$\langle \cos \phi \rangle = a^2 \frac{\partial}{\partial J}\int_a^\infty f(a')da' + O(L^{2-4Z}). \quad (34)$$

RG provides then an efficient method for evaluating $\omega_{\rm pl}$ via Eq. (34).

We proceed now to study correlations. We note first the correction in Eq. (34) $\langle \cos \phi \rangle_L - \langle \cos \phi \rangle \sim L^{2-4Z}$ [the upper limit in $\int^L f(a')da'$ gives the same exponent as can be seen from Sec. IV]. This correction determines the decay rate of the correlation function, by considering the second derivative $\partial^2 \mathcal{F}/\partial J^2 \sim (\partial/\partial J)\int \mathcal{D}\phi \cos \phi_0(0) e^{-H}/\mathcal{Z}$. This involves a $\cos \phi_n(\mathbf{r})$ correlation as well as $\langle \cos \phi \rangle^2$ from $\partial \mathcal{Z}/\partial J$, hence

$$\frac{\partial \langle \cos \phi \rangle}{\partial J} = \frac{1}{Ta^2}\sum_n \int d^2r \langle \cos \phi_0(0)\cos \phi_n(\mathbf{r})\rangle_c, \quad (35)$$

where $\langle \cos \phi_0(0)\cos \phi_n(\mathbf{r})\rangle_c = \langle \cos \phi_0(0)\cos \phi_n(\mathbf{r})\rangle - \langle \cos \phi \rangle^2$ vanishes at large $\mathbf{r}$. To reproduce the finite size correction L^{2-4Z} at $T>T_d$ the correlation must decay as $\langle \cos \phi_0(0)\cos \phi_0(\mathbf{r})\rangle_c \sim 1/r^{4Z}$.

In the coupled phase a approaches the correlation length ξ_d at which $J/T \approx 1$ becomes a strong coupling. The Hamiltonian can then be expanded as $\mathcal{H} \sim \sum_q (q^2 + \xi_d^{-2})|\phi(\mathbf{q},k)|^2$, keeping just the $q \to 0$ form. Hence for $r > \xi_d$ the system becomes Gaussian and the correlations decay exponentially. We conclude that

$$\langle \cos \phi_0(0)\cos \phi_0(\mathbf{r})\rangle_c \sim 1/r^{4Z},\ T>T_d,\ \sim e^{-r/\xi_d},\ T<T_d. \quad (36)$$

This distinctive behavior of the correlations serves as an additional identification of the phase transition.

We finally examine the validity of the high-temperature expansion which provides an easy estimate of $\langle \cos \phi \rangle$. We define $\langle \cdots \rangle_0$ as an average with respect to the $J=0$ system, so that

$$\langle [\phi_n(0) - \phi_n(\mathbf{r})]^2 \rangle_0 = T\frac{4\pi^2 d^2}{a^4}\int \frac{dk}{2\pi c_{44}^0(k)}\int \frac{d^2q(1-e^{i\mathbf{q}\cdot\mathbf{r}})}{4\pi^2 q^2(1+q^2/q_u^2)}, \quad (37)$$

where the c_{66} term is absorbed into $q_u^2 = 4\ln(a/d\sqrt{\pi})/\lambda_{ab}^2$ (at the dominant $k=\pi/d$ where c_{44}^0 is significantly softer). The k integration yields the first-order T_d^0 [Eq. (44) below] so that

$$\langle [\phi_n(0) - \phi_n(\mathbf{r})]^2 \rangle_0 = 4t\int \frac{d^2q}{\pi q^2(1+q^2/q_u^2)}(1-e^{-i\mathbf{q}\cdot\mathbf{r}}) = 8t\ln(rq_u),\ r>1/q_u, = -2t\, r^2 q_u^2 \ln(rq_u),\ r<1/q_u, \quad (38)$$

where $t=T/T_d^0$. Using the Gaussian average

$$\langle \cos \phi_n(0)\cos \phi_n(\mathbf{r})\rangle_0 = \exp\{-\langle [\phi_n(0) - \phi_n(\mathbf{r})]^2\rangle_0/2\} \quad (39)$$

and expansion of $\mathcal{Z}$ to first order in J/T we obtain

$$\langle \cos \phi \rangle = \frac{J}{Ta^2}\int d^2r' \langle \cos \phi_n(0)\cos \phi_n(\mathbf{r})\rangle_0 \approx \frac{\pi J}{Ta^2 q_u^2(2t-1)}; \quad (40)$$

the contribution of $r<1/q_u$ which becomes comparable at large t is omitted. To check the validity of Eq. (40) we note that it can also be obtained from the exact relation (35) taken as a perturbation in J, where $\langle \cos \phi \rangle \sim J^2$ is formally of higher order. However, this term is actually $\sim J^2L^2N$, hence the perturbation expansion formally fails at $L,N \to \infty$.

We note that within this naive perturbation expansion the correlation decays (incorrectly) to zero,

$$\langle \cos \phi^n(\mathbf{r})\cos \phi^n(0)\rangle \sim (rq_u)^{-4t} + O[(J/T)^2(rq_u)^{2-4t}] \quad (41)$$

with a finite contribution to $\langle \cos \phi \rangle$ in Eq. (40). We note also that the next order terms in J, while decaying more slowly, are still convergent in Eq. (40) for $t>1$. In fact the result (40), quite remarkably, reproduces the second-order RG result (up to a numerical prefactor) as found below. The reason is that the decay of Eq. (41) is actually correct for $\langle \cos \phi_0(0)\cos \phi_n(\mathbf{r})\rangle_c$ as in Eq. (36) (with $Z=t$ in weak coupling), which when substituted in Eq. (35) reproduces the form (40).

We summarize the salient features of the decoupling transition. (i) Relevancy of J corresponds to a broken gauge symmetry in the coupled phase, (ii) an order parameter that corresponds to (i) is Q of Eq. (28) or the Josephson current, and (iii) decay of correlations, such as $\langle \cos\phi_0(0)\cos\phi_n(\mathbf{r})\rangle_c$, is either exponential in the coupled phase or a power law in the decoupled phase.

IV. RG SOLUTION

The decoupling transition is driven by the singular response of the Josephson phase $b_n(\mathbf{r})$ in Eq. (19). The singularity is due to the long-range effect of an individual shift u_l^n which decays as $\nabla\alpha(\mathbf{r}-\mathbf{R}_l^n)\sim[\mathbf{r}-\mathbf{R}_l^n]^{-1}$ [see Eq. (18)]. The contributions of many such small displacements at a given location $\mathbf{r}$ result in a divergent response at the decoupling transition. The RG method is designed to handle such divergences and avoid the pitfalls of naive perturbation expansions.

A. First-order RG

The RG method proceeds by integrating out slices of high momentum shells $\Lambda-d\Lambda<q<\Lambda$, and the momentum cutoff Λ is successively reduced; initially $\Lambda=Q_0$. The field $\phi(\mathbf{q},k)$ is then decomposed as $\phi(\mathbf{q},k)=\zeta(\mathbf{q},k)+\chi(\mathbf{q},k)$ where $\zeta(\mathbf{q},k)$ carries momenta in the range $\Lambda-d\Lambda<q<\Lambda$ while $\chi(\mathbf{q},k)$ has momenta $q<\Lambda-d\Lambda$. In this subsection we analyze the phase transition by using the first-order equation in J. Expansion of Eq. (24) to first order in J and averaging on the high momentum shell yields

$$\langle\cos[\zeta_n(\mathbf{r})+\chi_n(\mathbf{r})]\rangle_\zeta=\cos\chi_n(\mathbf{r})\left(1-\frac{1}{2}\langle[\zeta_n(\mathbf{r})]^2\rangle\right). \tag{42}$$

Defining

$$G_b^{-1}(q,k)=\frac{q^2}{8\pi d}\frac{T}{g(q,k)}$$

we obtain $\langle[\zeta_n(\mathbf{r})]^2\rangle=d\int(dk/2\pi)g(\Lambda,k)d\Lambda/\Lambda$. Rescaling $a\to a+da(da/a=d\Lambda/\Lambda))$ leads to 1st order RG, i.e., it identifies the change in the coefficient y of the cos term, with the initial value $y_0=J/T$, as

$$\frac{dy}{y}=\left[1-d\int\frac{dk}{2\pi}g[\Lambda(x),k]\right]\frac{dx}{x}, \tag{43}$$

where $x=Q_0^2/\Lambda^2$ is in the range $1<x<\infty$. For a continuous transition the limiting $g(\Lambda\to 0,k)$ can be taken and the vanishing of the right-hand side in Eq. (43) identifies the decoupling transition temperature (which is independent of y_0)

$$T_d^0=\frac{4a^4}{d^2}\left[\int\frac{dk}{c_{44}^0(k)}\right]^{-1}. \tag{44}$$

This defines the units of our temperature variable t,

$$t=T/T_d^0 \tag{45}$$

and Eq. (43) has then the form (31) with $Z=t$.

The asymptotic solution of Eq. (43) is $y(x)=y_0x^{1-t}$. For $t>1$ the asymptotic $y(x)$ vanishes on long scales $x\to\infty$, hence the meaning of decoupling is that the Josephson coupling vanishes on long scales. For $t<1$ the coupling $y(x)$ increases, RG stops then when x reaches $x_d=(\xi_d/a)^2$ where strong coupling $y(x)\approx 1$ is achieved; this identifies a correlation length

$$\xi_d\approx a(y_0)^{1/[2(t-1)]}. \tag{46}$$

An explicit form for T_d^0 can be derived by noting the significant softening of $c_{44}^0(k)$ at $k>1/a$ which implies that the k integration in $g(\Lambda,k)$ is dominated by $k\approx\pi/d$. Hence we replace in Eq. (15) $\ln[(1+k_z^2/Q_0^2)/(1+\xi^2k_z^2)]\to 2\ln(a/d\sqrt{\pi})$, resulting in

$$G_b(q(x),k)=da^2\frac{4xt\sin^2(kd/2)}{T\left(1+\frac{1}{4gx}\right)}, \tag{47}$$

$$g(q(x),k)=\frac{2t\sin^2(kd/2)}{1+\frac{1}{4gx}} \tag{48}$$

so that

$$d\int\frac{dk}{2\pi}g[\Lambda(x),k]=\frac{t}{1+1/(4gx)}. \tag{49}$$

T_d^0 and the parameter[15] g are

$$g=\frac{a^2}{4\pi\lambda_{ab}^2}\ln\frac{a}{d\sqrt{\pi}},$$

$$T_d^0=g\tau=\frac{\tau a^2\ln(a/d\sqrt{\pi})}{4\pi\lambda_{ab}^2}. \tag{50}$$

Note that $1/4gx=q^2/q_u^2$ where q_u is defined below Eq. (37). A continuous transition is determined by the $x\to\infty$ behavior, hence Eq. (49) $\to t$ and the critical point is at $t=1$. We will examine below the possibility of a first-order transition, hence in general we keep $\sim 1/x$ terms. The solution for Eq. (43) is then

$$y(x)=y_0x\left(\frac{1+4g}{1+4gx}\right)^t \tag{51}$$

and the phase transition is indeed at $t=1$.

B. Second-order RG

We proceed to study second-order RG. Our main objective in this subsection is to see if RG can reproduce a first-order transition as proposed within the SCHA method.[10]

The RG procedure for a Hamiltonian of the type (23) has been derived in Appendix A of Ref. 22 up to second order in J. In this process new terms in the effective Hamiltonian are generated so that the partition sum has the form

$$Z = \int \mathcal{D}\phi \exp\left[-\frac{1}{2}\int \frac{d^2\mathbf{q}dk}{(2\pi)^3} G_R^{-1}(\mathbf{q},k)|\phi(\mathbf{q},k)|^2 + \int \frac{d^2\mathbf{r}}{a^2}\{y\cos[\phi_n(\mathbf{r})] + v\cos[\phi_n(\mathbf{r}) + \phi_{n+1}(\mathbf{r})]\}\right], \tag{52}$$

where we define

$$G_R^{-1}(q,k) = \frac{q^2}{8\pi d}\left(\frac{1}{g(q,k)} + h_0 + h_1\cos kd\right). \tag{53}$$

The new variables generated by RG, $v(x), h_0(x), h_1(x)$, are cutoff dependent with initial values of $v_0(1)=h_0(1)=h_1(1)=0$. Note that the renormalization of h^0 and h^1 is equivalent to renormalization of c_{44}^0. The recursion relations to second order in y are[22]

$$dy = [y(1-X_0) + yv(X_0+X_1)]dx/x,$$

$$dh_0 = [y^2X_0 + 4v^2(X_0+X_1)]dx/x,$$

$$dv = \left[v(1-2X_0-2X_1) - \frac{1}{4}y^2X_1\right]dx/x,$$

$$dh_1 = [4v^2(X_0+X_1)]dx/x, \tag{54}$$

where $X_n, n=0,1$ are h_0, h_1 and x dependent,

$$X_n = d\int \frac{dk}{2\pi}\frac{\cos(nkd)}{1/g(x,k) + h_0 + h_1\cos kd}. \tag{55}$$

We have absorbed factors γ, γ' of order 1 in the definitions of y, v which depend on the cutoff smoothing procedure;[22] the initial value of y is then $y(1)=\gamma' y$. Equations (54) are to be integrated from their initial values. To first order in y we rederive Eq. (43) above,

$$d\ln y = [1 - X_0(x, h_0 = h_1 = 0)]dx/x. \tag{56}$$

Before presenting numerical solutions for Eqs. (54), it is instructive to consider a simple situation where v and h_1 are neglected. This is a reasonable approximation since we eventually find that $v < y$ and $h_1 < h_0$. The RG equations are then

$$dy = y[1 - X_0(x)]dx/x,$$

$$dh_0 = y^2X_0(x)dx/x, \tag{57}$$

where [using the approximate form for the ln, as above Eq. (47)]

$$X_0(x) = d\int \frac{dk}{2\pi}\frac{1}{\frac{1+1/(4gx)}{2t\sin^2(kd/2)} + h_0(x)}. \tag{58}$$

We consider first the asymptotic solution at $x\to\infty$ in the regime where y is relevant, i.e., the coupled phase. Integrating the first equation of Eq. (57) we obtain

$$\ln\frac{y}{y_0} = \ln x - \int_1^x X_0(x')\frac{dx'}{x'}. \tag{59}$$

We claim that the second term converges, hence the parameter s

$$s = \int_1^\infty dx\frac{X_0(x)}{x} = d\int \frac{dk}{2\pi}\int_1^\infty dx \frac{1}{\frac{x+1/4g}{2t\sin^2(kd/2)} + xh_0(x)} \tag{60}$$

defines the asymptotic form of y,

$$y = y_0 x e^{-s}. \tag{61}$$

The RG equations are valid only up to $y\approx 1$, i.e., for a small y_0 up to a large $x_d=(\xi_d/a)^2$, but not infinite. Equation (60) therefore assumes that by formally extending Eq. (57) to $x\to\infty$ the integration range between ξ_d and ∞ is negligible.

We note that the $h_0(x)$ term represents an additional mass term in the propagator $G_R(q,k)$, Eq. (53) if $h_0(x)\sim x$. The $xh_0(x)$ term in Eq. (60) is then $\sim x^2$ and the integral is convergent. In the SCHA method such a mass term serves as a variational parameter and an analogous equation to Eq. (60) is derived in the next section. The essential point here is that $xh_0(x)$ is $\sim x^2$ only asymptotically while its scale dependence at finite x can be different, resulting in a different critical behavior. The scale dependence of the "mass" $h_0(x)/x$ is a feature which is beyond either first order RG or SCHA.

To complete the argument we need to show that $h_0(x)$ increases with x justifying the convergence of Eq. (60). Assuming that $h_0(x)$ increases with x, we can use $X_0\sim 1/h_0$ to yield from Eqs. (57) and (61) that indeed $h_0\approx y\sim x$. [For $x < x_d$ more terms in the the denominator of Eq. (58) need to be kept, modifying the way h_0 increases with x.]

We proceed now to solve the RG equations (57) in general form. Integrating Eq. (58) we obtain an explicit form

$$X_0 = \frac{t}{1 + th_0 + \frac{1}{4gx}} f(h_0,x,t), \tag{62}$$

where

$$f(h_0,x,t) = \frac{1}{b}\left(1 - \sqrt{\frac{1-b}{1+b}}\right)$$

and $b=th_0/[1+1/(4gx)+h_0t]$. The function $f(h_0,x,t)$ varies slowly between $0.84 < f(h_0,x,t) < 1$.

The RG Eqs. (57) for y and h_0 become

$$dy = y\left(1 - t\frac{f(h_0,x,t)}{\left(1 + th_0 + \frac{1}{4gx}\right)}\right)\frac{dx}{x},$$

$$dh_0 = t\frac{y^2 f(h_0,x,t)}{1 + th_0 + \frac{1}{4gx}}\frac{dx}{x}. \tag{63}$$

If the $1/(4gx)$ term in Eq. (63) is neglected and $f(h_0,x,t)=1$ is taken, Eq. (63) is equivalent to the Kosterlitz-

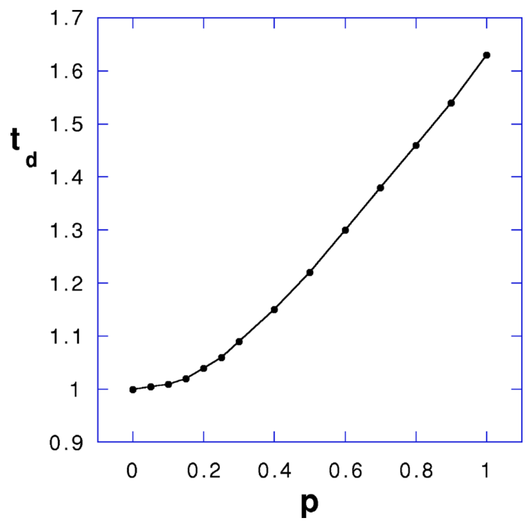

FIG. 1. (Color online) The decoupling temperature $t_d(p) = T_d(p)/T_d^0$ derived from the numerical solution of Eq. (63) with $4g=0.0001$.

Thouless equations[22] which show that the critical temperature is enhanced by a factor $1+y_0$ and that $y \sim x$ when y is relevant. The presence of the $1/4gx$ term leads, however, to a more significant enhancement which is measured by a parameter p,

$$p = \sqrt{\frac{Ty_0}{2\tau g^2}} = \sqrt{\frac{ty_0}{2g}} \tag{64}$$

measuring the ratio of two small parameters y_0 and g. It is also useful to express p in terms of the Josephson length $\lambda_J = \Phi_0 a\sqrt{d}/(4\lambda_{ab}\sqrt{J\pi^3})$, i.e., $p=(8\pi)^{-1/2}a/(g\lambda_J)$.

In the Appendix we derive a form for the critical temperature which yields a proper p dependence for both small and large p,

$$T_d = (1+2p^2)g\tau, \; p \ll 1, \tag{65}$$

$$T_d = \frac{3}{2}g\tau p, \; p \gg 1. \tag{66}$$

We have solved Eq. (63) numerically and the results for T_d are shown in Fig. 1. The p dependence is indeed significant, becoming linear at high p; in the range $1 \lesssim p < 1000$ we find $t_d = 0.95p$. Thus $T_d \sim 1/B$ [Eq. (50)] at $p \ll 1$ while $T_d \approx (a/\lambda_J)\tau \sim 1/\sqrt{B}$ at $p \gg 1$. We note also the significant enhancement in the value of T_d in the latter case, i.e., $T_d \gg T_d^0$. We note that the RG expansion is valid for $y_0 \ll 1$, which limits Eq. (66) [by inserting it in Eq. (64)] to $1 \ll p \ll 1/g$.

At $T < T_d$ we find that the variable y first increases, then decreases, corresponding to weakening of the $1/4gx$ term, and finally increases up to $y \approx 1$ at the scale $x = x_d = (\xi_d/a)^2$ where we should stop the renormalization process. The temperature dependence of x_d is shown on Fig 2. We see that the correlation length $\xi_d \to \infty$ as $T \to T_d$ which shows that the phase transition is a continuous one. We note that the early estimate of Glazman and Koshelev[9] of the decoupling temperature gives a result similar to Eq. (66). They derive a

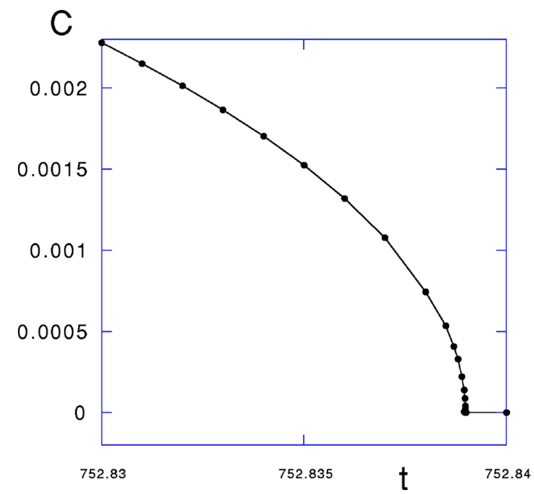

FIG. 2. (Color online) The temperature dependence of the correlation length ξ_d in terms of $C=[1+2\ln(\xi_d/a)]^{-1}$ near the decoupling transition temperature $t_d = T_d/T_d^0 = 752.839$. The numerical solution of Eq. (63) uses $4g=0.0001$ and initial conditions $y_0 = 0.01, h_0 = 0$, .

condition for large fluctuations $\langle\phi^2\rangle$ which by itself does not prove a phase transition; furthermore the estimated critical temperature vanishes with p, i.e., it is incorrect at $p \ll 1$. The large fluctuation condition is close in spirit to the SCHA method and is further discussed in Sec. V.

We present now numerical solutions of the full RG equations (54) with X_0 and X_1 given by Eq. (55) in Figs. 3 and 4, for the same initial conditions as in Fig. 2 [$y_0=0.01, h_0(x=1)=0$] and $v_0=0, h_1(x=1)=0$. We choose $4g=0.0001$ and these initial conditions since in this case the SCHA method (see Sec. IV) yields a first-order transition.

Figures 3 and 4 show the projected solution on the $y-h_0$ and $y-v$ planes, respectively. We find that $t_d=825.7$; for $t>t_d$ both the y and v variables vanish asymptotically, while at $t<t_d$ both y and v are relevant. The resulting correlation

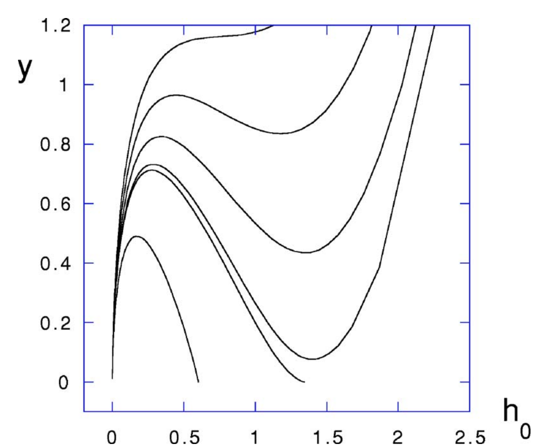

FIG. 3. (Color online) The numerical solution of the RG Eqs. (54) with $4g=0.0001$ and initial conditions $y_0=0.01$ and $h_0=h_1=0$, projected on the y-h_0 plane for different temperatures near the temperature of the decoupling transition $t_d=T_d/T_d^0=825.7$. A higher curve corresponds to a higher t, i.e., the two lower curves have $t<t_d$ while the others have $t>t_d$.

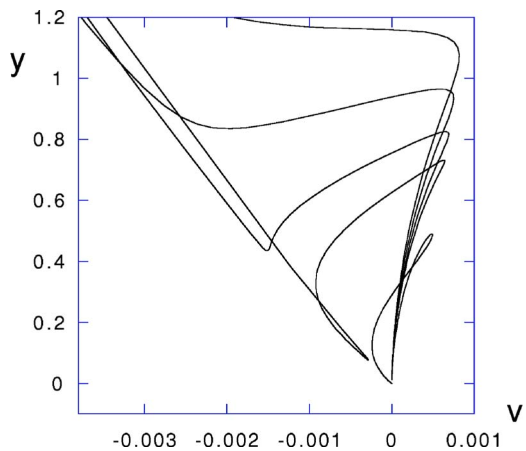

FIG. 4. (Color online) Same as Fig. 3 projected on the y and v plane.

length diverges at t_d, similar to Fig. 2, i.e., the transition is continuous. We have examined the transition also by varying the initial y_0, v_0; the correlation length was always found to diverge at $T \to T_d$ defining a continuous type phase transition.

Another scenario for a 1st order transition is via changing the initial value of v_0. Assuming a flow into strong renormalized y_r, v_r the free energy is dominated by

$$\mathcal{F}_r = \sum_n [-y_r \cos(\phi_n) - v_r \cos(\phi_n + \phi_{n+1})]. \quad (67)$$

The minimum at $\theta = \theta_n = \theta_{n+1}$ changes from $\theta = 0$ to $\cos\theta = -y_r/4v_r$ at large a negative $v_r, v_r < -y_r/4$. This hints at a first-order transition at some initial negative v; this is not the decoupling transition, but rather a transition within the coupled phase .

To emphasize the asymptotic forms we have integrated the RG equations up to $\sqrt{y^2+v^2} = 10^3$ and show in Fig. 5 the

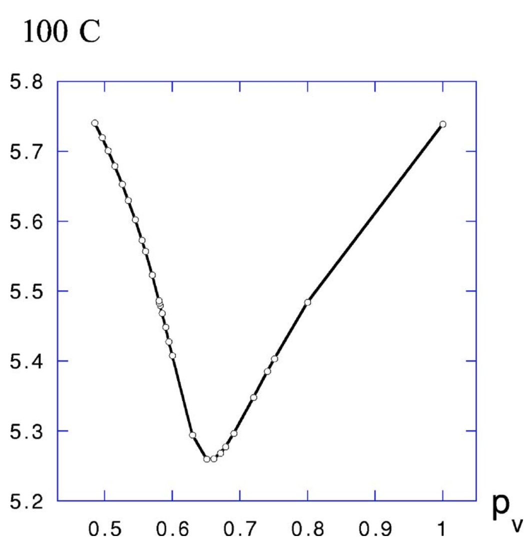

FIG. 5. (Color online) The correlation length in terms of $C = [1 + 2\ln(\xi_d/a)]^{-1}$ for $t = 0.5$ and $p = 1$ as function of $p_v = \sqrt{t|v_0|/2g}$ with $v_0 < 0$. The cutoff on the RG integration of Eq. (54) is $\sqrt{y^2+v^2} = 10^3$.

corresponding correlation length. For these parameters, the asymptotic v becomes negative above $p_v = \sqrt{t|v_0|/2g} = 0.5385$ (with $v_0 < 0$). The curve in Fig. 5 is continuous at this p_v since x_d is dominated by $y \gg v$ in the asymptotic regime. One needs to further increase $|v_0|$ until the asymptotic v and y values become comparable. In fact at $p_v = 0.65$ we observe a marked change in slope for $x_d(p_v)$ in Fig. 5. The asymptotic form $y \sim x^{\alpha}$ is found with α decreasing from 1 as p_v increases, saturating at $\alpha = 1/2$ when $p_v > 0.65$. Therefore, a first-order transition is possible within the coupled phase, associated with the relative strength of the renormalized y and v variables. The transition occurs when the initial v_0 is sufficiently negative.

V. PLASMA RESONANCE

We show here the relation $\omega_{\rm pl} \sim \langle \cos\phi \rangle$ and then apply Eq. (34) to evaluate $\langle \cos\phi \rangle$. In presence of a weak time dependent electric field $E(t)$ in the direction perpendicular to the layers the Josephson relation imposes a time dependent addition $\delta\phi_n(t)$ to the Josephson phase. The kinetic energy has the form

$$E_K = \epsilon_0 \int \frac{E^2}{8\pi} d^3r = \frac{\epsilon_0 \hbar^2}{32\pi e^2 d} \sum_n \int d^2r \left(\frac{d\delta\phi_n(t)}{dt} \right)^2, \quad (68)$$

where ϵ_0 is a dielectric constant. Expanding the Josephson coupling $-(J/a^2)\Sigma_n \int d^2r \cos[\phi_n(\mathbf{r}) + \delta\phi_n(t)]$ yields to second order $\frac{1}{2}(J/a^2)\langle \cos\phi \rangle [\delta\phi_n(t)]^2$ (the 1st order term has $\langle \sin\phi \rangle = 0$). This form neglects the possible time dependence of the Josephson term, e.g., dynamics of pancake vortices which are assumed to be slow on the scale of ω_{pl}. In particular the "phase slip" frequency was shown[12] to be much smaller than $\omega_{\rm pl}$. The plasma frequency is then

$$\omega_{\rm pl}^2 = \frac{16\pi e^2 dJ}{\epsilon_0 \hbar^2 a^2} \langle \cos\phi \rangle. \quad (69)$$

We proceed to evaluate $\langle \cos\phi \rangle$ from Eq. (34). Within second-order RG the contribution to the free energy[22] has the form of Eq. (30), i.e., $d\mathcal{F} = -NL^2 f(x)dx$ with

$$f(x) = \gamma' T\{y^2(x)X_0(x) + 2v^2(x)[X_0(x) + X_1(x)]\}/x^2. \quad (70)$$

We are mainly interested in $T > T_d$ where $v \ll y$ (see Fig. 4) so that we can use the truncated Eqs. (57). We use here the solution (A1) for either $p \ll 1$ or $p \gg 1$, written as

$$y(x) = y_0 x \left(\frac{1 + 4gt/Z}{1 + 4gtx/Z} \right)^Z, \quad (71)$$

where $Z = t/(1 + th_0^{\infty})$ and in general $Z = Z(t, J)$. The asymptotic form is $\sim x^{1-Z}$ so that $Z(t = t_d) = 1$ identifies the transition temperature, e.g., in first-order RG $Z = t$ and (71) reduces to Eq. (51). Using $X_0(x) = 4gtx/(1 + 4gtx/Z)$ and (71), Eq. (34) finally yields

$$\langle \cos\phi \rangle = \gamma' \frac{\partial}{\partial J} \frac{J^2 \tau}{2T^2} \frac{Z}{2Z - 1}, \quad (72)$$

where $tg = T/\tau \ll 1$ is assumed, corresponding to our requirement that T is well below melting. In particular for the case

$p \ll 1$, which is relevant for BSSCO,[6,7] we have $Z=t$ and

$$\langle \cos \phi \rangle = \gamma' \frac{J}{4gT} \frac{1}{2t-1} \tag{73}$$

which can also be derived directly with Eq. (51); at high temperatures $2t \gg 1$ we obtain $\langle \cos \phi \rangle = \gamma' J\tau/8T^2$. note that Eq. (73) is reproduced by the high temperature expansion Eq. (40) up to a prefactor $4\gamma'$. While the latter expansion is in general deficient, for evaluating $\langle \cos \phi \rangle$ it is reasonable, as discussed below Eq. (41).

Our main result for the decoupled phase in $p \ll 1$ systems is Eq. (73). In comparison, the melted phase where individual pancakes are uncorrelated has a correlation length of $\sim a$, so that $\langle \cos \phi_0(0) \cos \phi_n(\mathbf{r}) \rangle_c \approx e^{-r/a}$ is a plausible guess, hence from Eq. (35) we have $\langle \cos \phi \rangle \approx J/2T$; this form with a prefactor of order 1 was confirmed by simulations.[12] Hence in the decoupled phase $\langle \cos \phi \rangle$ is larger by a factor $\sim \tau/T$; furthermore, since $J \sim 1/B$ (J/a^2 is B independent) in the melted phase $\langle \cos \phi \rangle \sim 1/TB$ while in the decoupled phase it is $\langle \cos \phi \rangle \sim 1/[BT(2t-1)]$ or $\sim 1/BT^2$ not too close to decoupling. Thus the temperature dependence of ω_{pl} can distinguish between decoupled and liquid phases.

VI. THE SCHA METHOD

In this section we derive the decoupling transition within the variational SCHA method, reproducing the results of Ref. 10. In particular, this method results in a first-order transition at large p. We compare the method to that of second-order RG and show where the deficiency of SCHA originates.

The SCHA proceeds by searching for the optimal Gaussian Hamiltonian of the form

$$\mathcal{H}_0 = \frac{1}{2} \int_{\mathbf{q},k} \sum_{i,j} G_s^{-1}(q,k) \phi(\mathbf{q},k) \phi^*(\mathbf{q},k) \tag{74}$$

so that $G_s(q,k)$ is determined by minimization of the variational free energy

$$F_{\text{var}} = F_0 + \langle H - H_0 \rangle_0,$$

where the averaging as well as F_0 correspond to $\mathcal{H}_0$. F_{var} is then

$$\mathcal{F}_{\text{var}} = \frac{1}{2} \int_{q,k} \{-\ln G_s(q,k) + [G_s^{-1}(q,k) - G_b^{-1}(q,k)] G_s(q,k)\} - \frac{J}{a^2} e^{-(1/2)\int_{q,k} G_s(q,k)}, \tag{75}$$

where the $\ln G_s$ term corresponds to F_0 and we have used $\langle \phi^*(\mathbf{q},k) \phi(\mathbf{q},k) \rangle_0 = TG_s(q,k)$. The last term in Eq. (75) is the Josephson term with

$$\langle \cos \phi(\mathbf{r}) \rangle_0 = e^{-(1/2)T\int_{q,k} G_s(q,k)} = \exp(-s_v). \tag{76}$$

This defines a parameter s_v; the renormalized Josephson coupling is then Je^{-s_v}.

Minimizing Eq. (75) yields

$$G_s^{-1} = G_b^{-1} + \frac{J}{a^2 d} \exp(-s_v). \tag{77}$$

Using the form (47) and the variable x with $d^2q/(2\pi)^2 = -dx/(ax)^2$, Eqs. (76), (77) reduce to a self consistent equation for s_v

$$s_v = d \int \frac{dk}{2\pi} \int_1^\infty dx \frac{1}{\frac{x+1/4g}{2t \sin^2(kd/2)} + \frac{2J}{T} x^2 e^{-s_v}}. \tag{78}$$

This equation has exactly the same structure as that of Eq. (60) within second-order RG if the asymptotic form of RG variable $h_0(x) \to xy_0 e^{-s}$ is used. However the detailed $h_0(x)$ behavior is significant and can affect the critical properties; in fact, y and $h_0(x)$ are nonmonotonic.

We can perform the k integration in Eq. (78), neglecting the f type function as in Eq. (62) (i.e., replacing $0.84 < f < 1$ by $f=1$) leading to

$$s_v = \int_1^\infty dx \frac{4gt}{1 + 4gx + (4g)^2 p^2 x^2 e^{-s_v}} = \begin{cases} \dfrac{8gt}{\sqrt{D}} \arctan \left. \dfrac{2/x + 4g}{\sqrt{D}} \right|_\infty^1, & \text{if } D > 0, \\ \dfrac{4gt}{\sqrt{-D}} ln \left. \dfrac{2/x + 4g - \sqrt{-D}}{2/x + 4g + \sqrt{-D}} \right|_\infty^1, & \text{if } D < 0, \end{cases} \tag{79}$$

where $D = 16g^2[4p^2 \exp(-s_v) - 1]$ and p is defined in Eq. (64).

If the transition is continuous then s_v diverges near T_d so that the effective Josephson coupling $\sim e^{-s_v} \to 0$; Eq. (79) then yields $t_d = 1$. The RG result shows instead a weak p dependence even at small p as in Eq. (65) and Fig. 1.

At a first-order transition s_v is finite; anticipating a large $p, 4p^2 \exp(-s_v) \gg 1$ but $D \approx (8gp)^2 e^{-s_v} \ll 1$, Eq. (79) can be written as

$$s_v e^{-s_v/2} = \frac{\pi t}{2p}. \tag{80}$$

The product $s_v e^{-s_v/2}$ is bounded by $2/e$ at $s_v = 2$, hence as temperature approaches T_d from below s_v increases up to $s_v = 2$ but then jumps to $s_v = \infty$ in the decoupled phase, i.e., a first-order transition. The critical temperature is then

$$t_d = \frac{4}{\pi e} p, \ 1 \ll p \ll 1/g. \tag{81}$$

This result is similar to that from RG, Eq. (66), except that the slope is somewhat different. The significant difference is that RG yields a continuous transition even at large p.

At even larger p, where $p \gg 1/g, D \gg 1$, Eq. (79) yields

$$s_v e^{-s_v} = \frac{t}{4gp^2}. \tag{82}$$

As above, $s_v e^{-s_v}$ is bounded by $1/e$ at $s_v = 1$, hence a first-order transition at

$$t_d = \frac{4}{e} g p^2, \ p \gg 1/g. \tag{83}$$

The results $t_d=1$ for weak p and Eq. (83) for strong p are the results given in Ref. 10. The intermediate range Eq. (81) is not mentioned there, though the plotted decoupling fields $B_D(T)$ in their Fig. 1 are consistent with $B_D(T)\sim 1/T^2$ as from Eq. (81). Furthermore, Eq. (83) yields $T_d=(4gp)^2\tau/4e \gg \tau$ which is incompatible with the requirement that T_d is well below T_m.

It is interesting to note that the early estimate of Glazman and Koshelev[9] of the decoupling temperature gives a result similar to Eq. (81) or (66). Within this estimate the cos ϕ term in Eq. (23) is expanded and the condition of large fluctuations $\langle\phi^2\rangle\approx 1$ with $\langle\phi^2\rangle=T\int_{q,k}[G_b^{-1}(q,k)+J/a^2]^{-1}$ yields T_d. (This condition indicates decoupling, though by itself does not prove a phase transition.) The result is then the same as Eqs. (76), (77) with $s_v\approx 1$, therefore it yields indeed a result close to that of Eq. (81).

Our main result in this section is to show the formal similarity between SCHA and second-order RG as well as an important difference, i.e., the mass term which is generated by RG is scale dependent. Both methods show significant enhancement of T_d with increasing Josephson coupling, however the transition remains continuous in the RG solution.

VII. CONCLUSIONS

In recent experiments on BSCCO (Refs. 2 and 3) the phase diagram has shown a number of low temperature phases. Most of these transitions are disorder driven by either bulk pinning or by surface barriers. In particular the possibility that the second peak transition is a disorder driven decoupling has been suggested.[14,17] The significant reduction of the Josephson plasma resonance at the second peak supports a decoupling scenario,[6,7] however, a conclusive signature for decoupling has not been shown so far.

The signature of decoupling is that translational order is maintained, though with softer tilt modulus, while superconducting order is lost, i.e., $Q=0$ [Eq. (28)] and the critical current in the c direction vanish at $T>T_d$. An additional signature is the power law decay of the Josephson correlation at $T>T_d$. We find that the decoupling transition temperature is $T_d\sim 1/B$ at low fields [T_d^0 of Eq. (50)] while it changes to $T_d=0.95T_d^0 p\sim 1/\sqrt{B}$ at higher fields ($a\lambda_J\lesssim\lambda^2$) with significantly enhanced temperatures $T_d\gg T_d^0$.

We have shown that RG can be used to evaluate $\langle\cos\phi\rangle$ and hence the Josephson plasma frequency. In particular for weak coupling J, as in BSCCO, we find that $\omega_{pl}\sim 1/[BT(2T/T_d^0-1)]$, in contrast to a $\sim 1/BT$ behavior in the melted phase. This temperature dependence can serve to identify a decoupled phase.

In the present work we assume that *V-I* defects are not generated. Hence superconductivity is lost only in the c direction (i.e., $I_c=0$) while two-dimensional superconductivity is maintained parallel to the layers. Our neglect of *V-I* defects is in fact not justified, since they are generated at a lower temperature in the $J=0$ system,[15,16] i.e., at $T_d^0/8$. The true transition is a three-dimensional one in which both decoupling and the defect transition coalesce, similar to the $B=0$ scenario.[22] The actual transition temperature T_c is between T_d and the defect transition. It can be estimated by the temperature at which the correlation lengths of the defects ξ_{def} and ξ_d become comparable. Thus, e.g., if $\xi_{\rm def}>\xi_d$, the Josephson coupling is renormalized to strong coupling before the cos term feels the *V-I* defects. Since $\xi_{\rm def}\approx a\exp(E_c/T)$ (where $E_c\approx 0.2\tau$ is the pancake vortex core energy; if local lattice relaxation is included[24] then $E_c\approx 0.04\tau$) $\xi_{\rm def}$ is exponentially large, and T_c is close to T_d unless J is extremely small.

We expect for systems such as BSCCO or YBCO that decoupling affects mostly superconductivity in the c direction. The current-voltage relation parallel to the layers is expected then to be nonlinear,[14] except at very low currents where the few V-I defects would eventually lead to a linear Ohmic behavior. Similarly, the power law for the Josephson correlation would eventually, beyond the *V-I* spacing $\xi_{\rm def}$ decay exponentially.

In conclusion, we have studied the meaning and critical properties of the decoupling transition. On the theory side, in our view this is one of the few transitions of vortex matter which is fully understood. It remains to be seen if experiment can also provide clear realizations for this type of transition.

ACKNOWLEDGMENTS

This research was supported by The Israel Science Foundation founded by the Israel Academy of Sciences and Humanities. We thank A. Aharony, G. Zaránd, and S. Teitel for useful and valuable comments.

APPENDIX: EXPANSIONS FOR T_d

We present in this appendix an analytic expansion for the decoupling temperature T_d within the reduced set of Eq. (63) with $f(h_0,x,t)=1$. The results show a significant enhancement when the parameter p in Eq. (64) is large.

We consider $T>T_d$ where y flows to zero and h_0 reaches a finite asymptotic value h_0^∞, since the integration of dh_0 in Eq. (63) is convergent. We assume that the integration of the y equation is dominated by h_∞^0 and will examine below the validity of this assumption.

Integrating $y(x)$ in Eq. (63) with $h_0\to h_0^\infty$ yields

$$y = y_0 x\left(\frac{1+4g(1+th_0^\infty)}{1+4gx(1+th_0^\infty)}\right)^{t/(1+\mathrm{th}_0^\infty)}. \tag{A1}$$

We now substitute this $y(x)$ solution into the h_0 equation (63) and solve for h_0,

$$h_0(x) = \frac{p^4Z^2}{t^4(Z-1)(2Z-1)}\left(1-\frac{Z(2Z-1)}{(1+4gtx/Z)^{2(Z-1)}}+\frac{4Z(Z-1)}{(1+4gtx/Z)^{2Z-1}}-\frac{(t/p-1)(2t/p-1)}{(1+4gtx)^{2t/p}}\right), \tag{A2}$$

where h_0^∞ is also included in $Z=1/(1/t+h_0^\infty)$ and the important parameter p is defined in Eq. (64). Since $y\sim x^{1-Z}$ at large x, $Z=1$ defines the transition point.

We can now examine the consistency of replacing $h_0(x)$ by h_0^∞ in the y equation. The condition that $h_0(x)$ approaches h_0^∞ relatively fast is that the x dependent terms in Eq. (A2) are small at $x > 1/4gt$, i.e., Z is small (but $Z > 1$), hence p and h_∞^0 are large. It seems plausible then that our approximation is valid at $p \gg 1$. Alternatively, if $h_0(x) \ll 1$ then it has anyway a weak effect on the RG, i.e., the present derivation is valid at $p \ll 1$.

Equation (A2) shows that $h_0(x)$ converges to h_∞^0 if $Z > 1$. We now substitute $x \to \infty$ in Eq. (A2) and obtain a self-consistent equation for h_∞^0, which for the variable Z becomes a cubic equation

$$Z^3 - \frac{2+3/t}{(p/t)^4 + 2/t} Z^2 + \frac{3+1/t}{(p/t)^4 + 2/t} Z - \frac{1}{(p/t)^4 + 2/t} = Z^3 + a_2 Z^2 + a_1 Z + a_0 = 0. \tag{A3}$$

This cubic equation has solutions $Z > 1$ only if the condition $D(t) < 0$ is satisfied, where

$$D(t) = \frac{1}{27} a_1^3 - \frac{1}{6} a_0 a_1 a_2 + \frac{1}{27} a_0 a_2^3 - \frac{1}{4 \times 27} a_1^2 a_2^2 + \frac{1}{4} a_0^2. \tag{A4}$$

Therefore, $D(t) = 0$ corresponds to $Z = 1$ and defines the temperature of the phase transition T_d as given in Eqs. (65), (66).

[1] For a review see P. H. Kes, J. Phys. I **6**, 2327 (1996).
[2] B. Khaykovich, E. Zeldov, D. Majer, T. W. Li, P. H. Kes, and M. Konczykowski, Phys. Rev. Lett. **76**, 2555 (1996); B. Khaykovich, M. Konczykowski, E. Zeldov, R. A. Doyle, D. Majer, P. H. Kes and T. W. Li, Phys. Rev. B **56**, R517 (1997).
[3] D. T. Fuchs, E. Zeldov, T. Tamegai, S. Ooi, M. Rappaport, and H. Shtrikman, Phys. Rev. Lett. **80**, 4971 (1998).
[4] K. Deligiannis, P. A. J. de Groot, M. Oussena, S. Pinfold, R. Langan, R. Gagnon, and L. Taillefer, Phys. Rev. Lett. **79**, 2121 (1997).
[5] N. Avraham, B. Khaykovich, Y. Myasoedov, M. Rappaport, H. Shtrikman, D. E. Feldman, T. Tamegai, P. H. Kes, M. Li, M. Konczykowski, K. van der Beek, and E. Zeldov, Nature (London) **411**, 451 (2001).
[6] T. Shibauchi, T. Nakano, M. Sato, T. Kisu, N. Kameda, N. Okuda, S. Ooi, and T. Tamegai, Phys. Rev. Lett. **83**, 1010 (1999).
[7] M. B. Gaifullin, Y. Matsuda, N. Chikumoto, J. Shimoyama, and K. Kishio, Phys. Rev. Lett. **84**, 2945 (2000).
[8] L. I. Glazman and A. E. Koshelev, Physica C **173**, 180 (1991).
[9] L. I. Glazman and A. E. Koshelev, Phys. Rev. B **43**, 2835 (1991).
[10] L. L. Daemen, L. N. Bulaevskii, M. P. Maley and J. Y. Coulter, Phys. Rev. Lett. **70**, 1167 (1993).
[11] For a review on the theory of vortex matter see G. Blatter, M. V. Feigel'man, V. B. Geshkenbein, A. I. Larkin, and V. M. Vinokur, Rev. Mod. Phys. **66**, 1125 (1995).
[12] A. E. Koshelev, Phys. Rev. Lett. **77**, 3901 (1996).
[13] Y.-H. Li and S. Teitel, Phys. Rev. B **47**, 359 (1993).
[14] B. Horovitz and T. R. Goldin, Phys. Rev. Lett. **80**, 1734 (1998).
[15] M. J. W. Dodgson, V. B. Geshkenbein, and G. Blatter, Phys. Rev. Lett. **83**, 5358 (1999).
[16] B. Horovitz and P. Le Doussal, Phys. Rev. Lett. **84**, 5395 (2000); Phys. Rev. B **71**, 134202 (2005).
[17] B. Horovitz, Phys. Rev. B **60**, R9939 (1999).
[18] B. Horovitz, following paper, Phys. Rev. B **72**, 024519 (2005).
[19] A. Morozov, B. Horovitz and P. Le Doussal, Phys. Rev. B **67**, 140505(R) (2003).
[20] W. E. Lawrence and S. Doniach, in *Proceedings of the Twelfth International Conference on Low Temperature Physics* (LT-12), Kyoto, 1970, edited by E. Kanda (Keigaku, Tokyo, 1971), p. 361.
[21] M. J. W. Dodgson, A. E. Koshelev, V. B. Geshkenbein and G. Blatter, Phys. Rev. Lett. **84**, 2698 (2000); H. Fanghor, A. E. Koshelev and M. J. W. Dodgson, Phys. Rev. B **67**, 174508 (2003).
[22] B. Horovitz, Phys. Rev. B **47**, 5947 (1993).
[23] T. R. Goldin and B. Horovitz, Phys. Rev. B **58**, 9524 (1998).
[24] E. Olive and E. H. Brandt, Phys. Rev. B **57**, 13 861 (1998).